



Late Quaternary Ice Cap Extent and Deglaciation, Húnaflóaáll, Northwest Iceland: Evidence from Marine Cores

Authors: Andrews, John T., and Helgadóttir, Gudrun

Source: Arctic, Antarctic, and Alpine Research, 35(2) : 218-232

Published By: Institute of Arctic and Alpine Research (INSTAAR),
University of Colorado

URL: [https://doi.org/10.1657/1523-0430\(2003\)035\[0218:LQICEA\]2.0.CO;2](https://doi.org/10.1657/1523-0430(2003)035[0218:LQICEA]2.0.CO;2)

BioOne Complete (complete.BioOne.org) is a full-text database of 200 subscribed and open-access titles in the biological, ecological, and environmental sciences published by nonprofit societies, associations, museums, institutions, and presses.

Your use of this PDF, the BioOne Complete website, and all posted and associated content indicates your acceptance of BioOne's Terms of Use, available at www.bioone.org/terms-of-use.

Usage of BioOne Complete content is strictly limited to personal, educational, and non - commercial use. Commercial inquiries or rights and permissions requests should be directed to the individual publisher as copyright holder.

BioOne sees sustainable scholarly publishing as an inherently collaborative enterprise connecting authors, nonprofit publishers, academic institutions, research libraries, and research funders in the common goal of maximizing access to critical research.

Late Quaternary Ice Cap Extent and Deglaciation, Húnaflóaáll, Northwest Iceland: Evidence from Marine Cores

John T. Andrews

Institute of Arctic and Alpine Research and
Department of Geological Sciences,
University of Colorado, Box 450, Boulder,
CO 80309, U.S.A.
andrewsj@spot.colorado.edu

Gudrun Helgadóttir

Marine Research Institute of Iceland,
Skúlagata 4, 101 Reykjavík, Iceland.
Gudrun@hafro.is

Abstract

The extent of the Last Glacial Maximum (LGM) and the timing of deglaciation around the Northwest Peninsula of Iceland are poorly understood. To provide information on these issues, we report sedimentological, foraminiferal, isotopic, and chronological data from marine piston cores B997-322PC, -323PC, -326PC1, and -326PC2 from a transect along Reykjafjardaáll/Húnaflóaáll, a large trough that extends from the north Iceland coast toward the shelf break, ca. 66.8°N and 20°W. Cores B997-322PC, -323PC, and -326PC1 recovered diamictos (stiff, pebbly muds) overlain by fine-grained, postglacial muds, with intermittent occurrences of iceberg-rafted clasts and volcanic shards. No glacial constructional features (moraines) were noted on the seismic profiles. In the outermost cores (B997-322PC and 323PC) the diamictos contained small but persistent numbers of foraminifera which gave dates between 25 and 44 ka B.P.; foraminifera are absent in the diamicton at the base of core B997-326PC1. ^{14}C dates immediately above the diamictos have ages of ca. 13 ka B.P., which we take to represent the date of deglaciation of Húnaflóaáll and the withdrawal of the ice margin to the adjacent Strandir coast. Foraminifera are used to construct a bio- and isotope stratigraphy of cores B997-322PC and 323PC. In the diamictos, the fauna is dominated by cold-water benthic foraminifera including *Elphidium excavatum* and *Cassidulina reniforme*; *Cassidulina neoteretis* is also a persistent component. In B997-322PC and -323PC the deglacial sequence is interrupted by an interval of IRD deposition, a dramatic reduction in foraminiferal numbers, and heavy $\delta^{18}\text{O}$ values; we equate this interval with the Younger Dryas cold event. Alternative working hypotheses are advanced for the origin of the diamictos and their importance to mapping the LGM ice extent. The 12-ky hiatus between the diamictos and the overlying marine muds indicates that the sequence is not conformable. The diamictos probably represent glacial-marine sediments overrun by late Weichselian ice streaming down the trough. The absence of a thick, deglacial sequence of glacial-marine sediments indicates a dramatic retreat of the ice cap to the present coast by ~ 13 ka B.P.

Introduction

Although Iceland lies in a pivotal position within the North Atlantic climate system (Lamb, 1979) (Fig. 1), it is only very recently that detailed evaluations of late Quaternary marine records are becoming available (Andrews et al., 2000; Eiriksson et al., 2000a; Jennings et al., 2000). A major unresolved issue is the extent of the glaciation of Iceland during the Last Glacial Maximum (LGM), especially the extent of ice on the Northwest Peninsula (Norrdahl, 1991) (Fig. 1). Our purpose is to present sedimentological, chronological, and faunal analysis of piston cores (B997-322PC, -323PC, -326PC1, and -326PC2) (Fig. 2) (henceforth 322PC) that were collected on a joint Iceland/U.S.A. research cruise (B997-) on the research vessel *Bjarni Saemundsson* (Helgadóttir, 1997). The basal dates from these cores gave uncorrected ages of $42,600 \pm 3050$ B.P. and $25,330 \pm 640$ B.P. (Andrews et al., 2000; Smith and Licht, 2000), suggesting that these cores might embrace ice sheet/ocean interactions during part of Marine Isotope Stage (MIS) 3 and the whole of MIS 2 and 1.

The focus of this paper is the description and interpretation of sediment sequences in these four cores, in particular the interpretation of pebbly muds (diamictos) that in 322PC and 323PC contain persistent numbers of benthic and planktonic foraminifera. Such

sediments could reflect (1) open-water glacial-marine conditions, (2) reworking of glacial-marine sediments by glacial ice, or (3) subglacial tills. The first situation would indicate that the sites were not glaciated, whereas the latter two options permit the covering of the sites by grounded ice. Thus there are two important questions associated with the core stratigraphies: (1) what is the origin(s) of the diamictos? (2) is the contact between diamictos and the fine-grained muds synchronous along the trough, and does it reflect deglaciation of the shelf? In this paper dates are usually expressed in units of ka B.P. or cal ka B.P. where the dates are calibrated. We use ky to represent a rate.

Background

The glacial and volcanic history of Iceland has become of regional significance owing to the recognition of Icelandic tephra in Greenland ice cores and in North Atlantic marine and lakes cores (Bjorck et al., 1992; Grönvold et al., 1995; Haffidason et al., 2000) and because the record of far-travelled sediments of Iceland origin appear to have some nonrandom relationship with abrupt events (e.g., Heinrich events) in the North Atlantic (Bond and Lotti, 1995; Elliott et al., 1998). However, the nearshore record of the extent and history

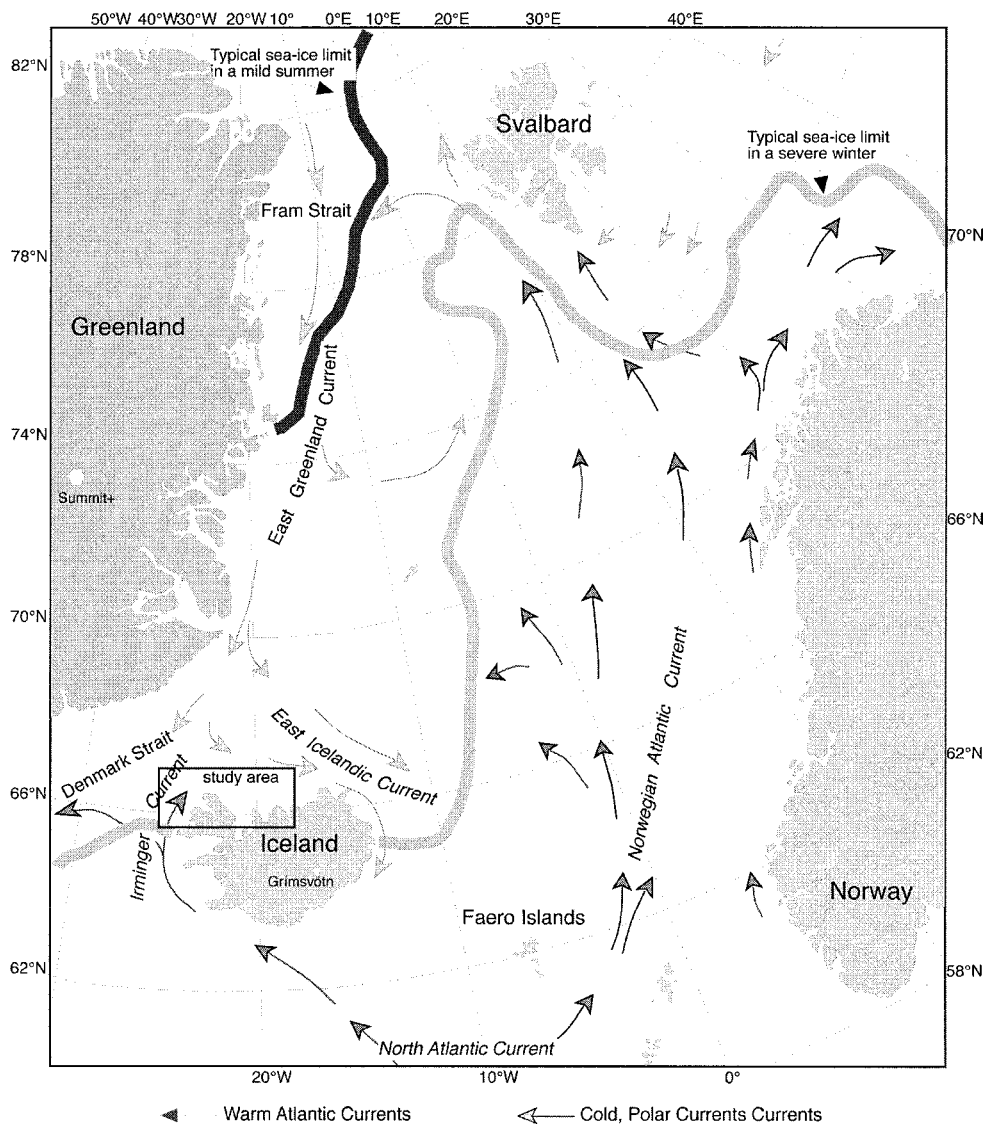


FIGURE 1. Surface currents in the northern North Atlantic and the location of this study on the Iceland margin (identified by the boxed-in area).

of glaciation and ice-rafting around Iceland is currently poorly documented, although significant efforts are now being directed toward this problem (Kristjansdóttir, 1999; Eiriksson et al., 2000a; Cartee Schoolfield, 2000; Jennings et al., 2000; Geirsdóttir et al., 2001, 2002).

Our paper deals with the interaction between the Iceland Ice Cap and the ocean at sites north and northeast of the Northwest Peninsula. This large peninsula is separated from the main bulk of the island by a narrow strip of land (Figs. 1 and 2). It is uncertain how the glaciation of the Northwest Peninsula is tied into the glacial history of the rest of Iceland (Norddahl, 1991) and whether there were refugia on coastal mountains (Rundgren and Ingolfsson, 1999). Was there a separate ice cap over the peninsula, or did it join with the main Iceland Ice Cap? In particular, the extent of glaciation during the LGM at roughly 22 cal ka B.P. is unknown (Ingolfsson, 1991; Eiriksson et al., 1997). Glaciological modeling is now starting to develop hypotheses of the variations in glacial extent across Iceland during the last glacial cycle. For example, Webb et al. (1999) indicate total ice coverage during the LGM. However, geomorphic reconstructions of the Iceland Ice Cap (Bourgeois et al., 2000; Stokes and Clark, 2001) suggest that the Northwest Peninsula hosted a separate ice center with an ice divide forming a broad U-shape, draining principally into Ísafjardardjúp (Fig. 1). Because of the limited accumulation area, the Northwest Peninsula

ice cap may not have extended to the shelf break. Indeed, research on the sediment history in Djúpall (Andrews et al., 2002c; Geirsdóttir et al., 2002) suggested that at the LGM, the ice stream in Ísafjardardjúp extended just beyond the mouth of this large fjord complex. Glacial-marine diamictons have been recovered in Djúpall (cores B997-338 and MD99-2264, Fig. 2) that provide a continuous history of deposition between 13 and 36 cal ka B.P. (Andrews et al., 2002c; Geirsdóttir et al., 2002). If this picture is correct, and it is supported by other facts such as very low marine limits at the tip of the Northwest Peninsula (Hjort et al., 1985), then it then raises the question of how far offshore could the Northwest Peninsula ice cap have extended seaward of the Strandir coastline, and was there a separate ice stream in Reykjafjarðaáll/Húnaflóaáll (Fig. 2).

There are also questions about the postulated LGM age of the Latra End Moraine, which lies at the shelf break, west of the Northwest Peninsula (Olafsdóttir, 1975; Syvitski et al., 1999). If this deposit is indeed older than the LGM (Andrews, in press) then symmetry and ice-sheet reconstructions indicate that ice may not have flowed completely along Reykjafjarðaáll/Húnaflóaáll on the way to the northern shelf break. Thus, the extent of ice during the LGM in Húnaflóaáll is presently uncertain, although on the basis of the two initial basal dates in 322PC and 323PC, Andrews et al. (2000) placed an ice margin landward of B997-323PC.

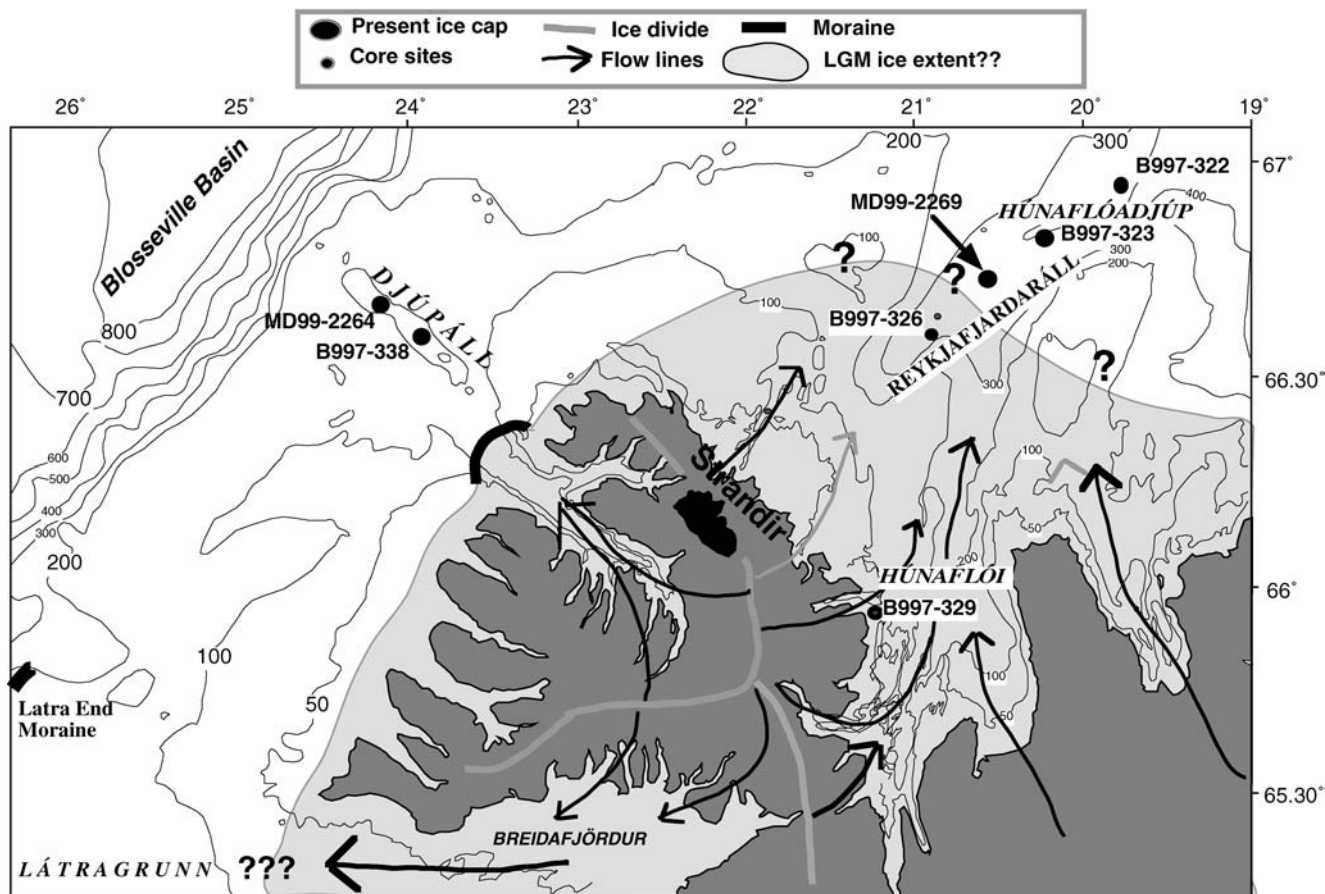


FIGURE 2. Place names, core locations and possible extent of the last glacial maximum (LGM) ice limit around the Northwest Peninsula of Iceland. Ice divides and flow lines are after Bourgeois et al. (2000), Geirsdóttir et al. (2002), and Andrews et al. (2002c).

Húnaflóaáll is a large trough that trends roughly south to north and thus angles away from the trend of the northeast coast of the Northwest Peninsula (Fig. 2). Where this trough meets Reykjafjarðaáll, the combined feature is called Húnaflóadjúp. Húnaflóadjúp attains maximum water depths of 400 to 500 m but becomes shallower at both its landward margin and seaward (Fig. 2). For Reykjafjarðaáll/Húnaflóaáll to be filled by an active outlet ice stream, there must have been an ice divide at the waist of the peninsula and a reasonable thickness of ice to promote flow to the north along Húnaflóadjúp (Bourgeois et al., 2000). There are, however, very few observations pertaining to ice extent and deglaciation of this northern area (Larsson, 1983; Hjort et al., 1985). The best estimate of the deglaciation of this part of the Northwest Peninsula is that it occurred sometime prior to 12 ka B.P. (Ashwell, 1996; Rundgren et al., 1997).

The area off northwest/north Iceland is critically situated with respect to ocean circulation (Malmberg, 1969, 1985; Stefansson, 1969a, 1969b; Lamb, 1979; Olafsson, 1999). Húnaflóaáll lies along one of the standard hydrographic transects made on a seasonal basis by the Marine Research Institute, Iceland. This transect recorded an abrupt switch from Atlantic Water to Polar Water in the 1960s associated with the Great Salinity Anomaly (Lamb, 1979; Malmberg, 1985; Dickson et al., 1988; Belkin et al., 1998). The warm Irminger Current moves up the west side of Iceland (Fig. 1); one branch splits and moves across the Denmark Strait and then southward, whereas the remainder is directed around the Northwest Peninsula and then moves eastward as the North Iceland Irminger Current (Hopkins, 1991). Farther seaward, the East Iceland Current, a branch of the East Greenland Current (Fig. 1), brings cold surface water and frequently heavy sea ice and a few

icebergs to north Iceland in extreme years (Stefansson, 1969a; Sigtryggsson, 1972). In 1997 our hydrographic casts indicated the presence of a shallow, thin cold layer underlying the surface coastal water. At depths >50 m, water temperatures decreased gradually toward 0°C at site 323PC. The upper 50 m of the water column shows a rapid (2‰) increase in salinity. Below 50 m, the high salinities (~34.9‰) suggest the presence of Atlantic Water and winter-cooled Atlantic Water at depths >200 m.

Core Sites and Seismic Stratigraphy

Cores 322PC and 323PC were collected from Húnaflóadjúp; 326PC1 and 326PC2 were collected on the landward side of the basin along Reykjafjarðaáll (Fig. 2). A 3.5-kHz system was employed to obtain estimates of sediment thickness and overall seismic stratigraphy (Helgadóttir, 1997; Andrews et al., 2000) (Fig. 3). Water depths varied from 397 to 351 m. The seismic data suggest that Húnaflóadjúp is occupied by a shelf sediment or drift deposit (McCave and Tucholke, 1986; Faugeres et al., 1999; Harris et al., 2001), with older sediment outcropping near the sea floor to the north and south of the drift (Fig. 3B). A well-defined seismic reflector lies deep (21 m) within the Quaternary section in the center of the basin. This reflector was cored at site MD99-2269 (Fig. 2) and shown to be the 9 ka B.P. Saksunarvatn tephra (Andrews et al., 2002a, 2002d). This reflector is near the surface at the margins of the trough, such sites of 323PC and 326PC (Fig. 3), but it is not obvious on the outer shelf near site 322PC. On the inner shelf at 329PC (Fig. 2) (Castaneda, 2001; Andrews et al., 2002d) the Saksunarvatn tephra occurs about 2.2 m below the seafloor—these

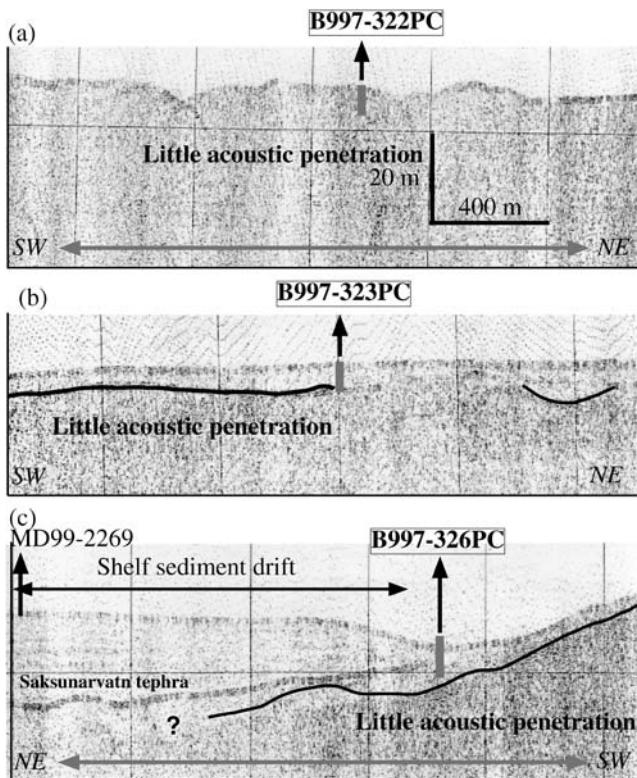


FIGURE 3. 3.5 kHz seismic lines from the B997 cruise showing (a): site of B997-322PC; (b): site of B997-323PC; and (c): site of B997-326 and MD99-2269—the strong reflector is correlated in core MD99-2269 with the Saksunarvatn tephra (Andrews et al., 2002d). The vertical and horizontal scales in (a) apply to all sections. The directions that the lines were taken are indicated, for example, southwest (SW) to northeast (NE).

relationships confirm that the main sediment drift accumulation in Húnaflóadjúp (Fig. 3) is post ~9 ka B.P.

At 322PC the sea floor is gently rolling, with a relief of 5 to 10 m. Little to no seismic penetration was achieved, suggesting a thin sediment cover over dense sediment or bedrock. At the site of 323PC, an internal reflector is close to the surface and has some limited (1 to 2 m) relief. Acoustically transparent sediment overlies the reflector, but the records are not good enough to determine much detail (Fig. 3). Immediately seaward of 326PC, over 30 m of sediment fills the basin, and one prominent reflector, the same as noted at 323PC, appears to crop out at or near the surface. Here it is clear that the reflector occurs above an additional 10 m or so of sediment that thins toward the core site (the ship drifted during the extraction of 326PC1 and 326PC2; see Table 1). During the 1999 cruise along Húnaflóaáll in the French research vessel *Marion Dufresne*, as part of an IMAGES V coring expedition, a 25m core (MD99-2269, Fig. 2) was recovered in the center of trough and penetrated the two main seismic reflectors. Our research indicates that the uppermost regional reflector is caused by deposition of the Saksunarvatn tephra at 9 ka B.P. ($10.18 \pm \text{cal ka B.P.}$) (Grönvold et al., 1995; Andrews et al., 2002d).

Sediment Cores: Methods

The resolution of the 3.5-kHz system was such that we are uncertain whether the “basement” is bedrock or acoustically “hard” sediment, such as a diamicton. We used both a 10-cm gravity corer, usually with a 2- to 3-m barrel, and a 6-m piston corer (PC) with a diameter of 7 cm. Our primary goal was to achieve the longest

(temporal) record, at the risk of low resolution. Cores 322PC, 323PC, and 326PC1, with lengths of ca 1.5 and 3 m (Table 1), penetrated stiff, pebbly sediments and indicate that at these sites at least, the acoustic basement is glacial or glacial-marine diamictons.

The cores were split, photographed, described, X-radiographed, and sampled for both sediments and foraminifera. We visually described the cores using a lithofacies code (Eyles et al., 1983). The primary lithofacies identified are massive, matrix-supported diamictons (Dmm) and fine-grained muds (F) (Figs. 4, 5). Sediment samples consisted of a 10.4-cc container that allowed the determination of wet and dry density. Other processes included determination of total organic carbon (TOC) and total carbonate with a Coulometer, mass magnetic susceptibility with a Bartington meter, and grain-size determinations using a long-bed Malvern laser system (Syvitski, 1991; Andrews et al., 2002b). The number of clasts >2 mm were counted in 2-cm vertical segments from X-radiographs (Grobe, 1987; Andrews et al., 1997).

The foraminiferal samples were washed through a 63- μm screen and then sieved at 105 μm and 1000 μm (Knudsen and Austen, 1996). We split the sand fraction into two using a microsplitter; we used one half for foraminiferal assemblages and numbers/g estimates and the half for sediment composition. We obtained sediment weights and expressed the foraminifera results as numbers/gram of sediment and as percentages of the total fauna. We based individual identifications on prior research and on surface collections made around Iceland (Helgadóttir, 1984; Weiner et al., 1999). We picked between 10 and 20 individuals of the polar planktonic foraminifera *Neogloboquadrina pachyderma* s for isotopic analyses. The samples were processed at the Woods Hole Oceanographic Institutes stable isotope laboratory supervised by R. Osterman.

We evaluated the composition of the sediment fraction in the 105 to 1000 μm fraction. Because of the high proportion of sand-size particles, we did not attempt an estimate of numbers/gram, but rather worked with percentage composition because of the potentially large error involved splitting the sample many times to achieve a 300 grain/slide coverage. We cast an even spread of material on a tray marked off in 1-cm² intervals. Samples were selected randomly for processing to avoid biases in the counting procedure. We used a binocular microscope at 40 \times power and counted between 200 and 300 grains, at randomly selected grid intersections. Sediment pellets were counted, but these were considered outside the sum; thus in any sample the total number of objects counted ranged between 300 and 500. We identified eight compositions, namely: bubble-wall clear ash, dark glassy or pumaceous ash, quartz, “red” grains, modified (abraded) basaltic grains, other rock fragments, foraminifera, and sediment pellets. The term “tephra” is used to describe a variety of grain shapes, colors, and compositions (Hafidason et al., 2000); we use it synonymously with “ash,” which is defined as volcanic materials <2 mm. The common element in the recognition of ash particles is that they possessed sharp, angular corners with no evidence of wear. In our usage (Figs. 4, 5), “lithics” included red grains, quartz, other, and modified basaltic grains. “Dark lithics” were principally basalts, also containing “glassy” grains, but these grains had subangular to subrounded (occasionally rounded) corners and overall shapes indicating moderate to substantial abrasion. For the first seven elements the counts were converted to percentages, whereas the sediment pellets were expressed as a percentage of the seven element count. Standard errors of the counts were computed using standard formulae (Hamilton, 1990). Because counts were converted to percentage data, with all sums hence equaling 100, in our multivariate analyses we used the log ratio transformation to avoid the closed array problem (Aitchison, 1986; Hamilton, 1990; Kovach, 1998). For our data analyses we used two main programs, StataTM (Stata, 1999) and Multivariate Statistical Programs (MVSP) (Kovach, 1998). In our analysis (see later) we

TABLE 1

Core locations and radiocarbon AMS dates (see Smith and Licht, 2000, for additional details on species, numbers, and $\delta^{13}C$)

Core Id: Lab. #.	Latitude and Longitude		water depth (m)		core length (cm)
	Depth (cm)	Date (uncorrected)	error \pm	weight (mg)	Material
	B997-322PC2 66°56.29' & 19°46.55'		357		161
AA-39957	8–10	1,900	60	4	mixed b
AA-32958	18–20	3,810	70	7.8	mixed b
AA-32959	38–40	11,970	130	3.6	mixed b
AA-32960	78–80	9,120	130	2.5	mixed b
AA-32961	136–140	>37,800		1.3	mixed b
AAAR-3887	162	42,600	3050	7.2	Mixed b & p
	B997-323PC 66°50.79' & 20°13.64'		397		292
AA-33633	37–38.5	8,520	110	5.8	mixed b & p
AA-34400	60	13,100	130	5.2	b
AA-32963	70–71	13,440	190	4.0	mixed b & p
AA-32964	88.7–91.2	>25,900		3.0	mixed b & p
AA-32965	238.7–241.2	>30,500		1.6	mixed b & p
AA-27763	292	25,330	640	6.1	Mixed b & p
	B997-326PC1 66°36.35' & 20°54.82'		358		297
AA-32966	10–12	3,690	70	3.8	mixed b
AA-34401	16–21	9,040	110	4.2	mixed b
AA-34402	108–114	9,580	100	5.0	mixed b
AA-40085	183	13,835	215	2.8	mixed b & p
AA-34403	196–200	23,570	340	4.7	mixed b
	B997-326PC2 66°36.33' & 20°55.43'		351		167
AA-34406	0–1	modern		5.2	mixed b
NSR-10785	50	1,570		29.1	<i>Dentalium</i>
AA-34405	74–76	6,810	80	12.1	gastropod
AA-33842	153	13,155	95		single species, <i>N. labradoricum</i>

p = planktic species.

b = benthic species.

plotted compositional ratios to discriminate between environments of deposition. For example, the ratio of lithics:lithics plus foraminifera is commonly used to designate a change between an ice-rafted debris dominated environment and more open (less or nonglacial) marine conditions (Bond and Lotti, 1995).

We picked individual tephra shards for elemental analysis. Some of these were processed at the Nordic Volcanological Institute, Iceland (Dr K. Grönvold); we also probed at the University of Colorado with a JEOL 8600 electron microprobe at 15 Kv accelerating voltage, 20 nanoAmp cup current and a 5 μ m beam. The results were standardized to a US Natural History Museum basaltic glass standard A99 (#113498). Data were reduced using the Bence Albee 1968 reduction procedure. 326PC2 had discrete ash units that were visible on opening the core, but in the other three cores there were changes in the relative composition of the sand-size fraction. The geochemical results from our analyses will be available on the NOAA data base.

Core Chronologies: AMS ^{14}C Dates and Tephtras

Details on the number of foraminifera species dated and on the sample $\delta^{13}C$ are given in Smith and Licht (2000). In order to obtain samples of sufficient mass we usually had to combine all species. Because these sites from relatively shallow waters (<400 m) it is unlikely that samples from near-surface and benthic species would have greatly varying ages, and $\delta^{13}C$ variations are minimal.

We have not adjusted the radiocarbon dates on Table 1 and Figures 4 and 5 for an ocean reservoir correction because there is discussion as to what this correction should be at present (Håkansson, 1983; Hafliðason et al., 2000), and both spatial and temporal variations are expected (Bard et al., 1994; Hagen, 1999; Voelker et al., 1998;

Voelker, 1999; Eiriksson et al., 2000b). Based on a comparison between terrestrial age estimates (Hafliðason et al., 2000; Wastl et al., 1999) and our marine dates on the Saksunarvatn ash at sites south and west of 326PC (Andrews et al., 2002d), it appears that for the last 9000 ^{14}C yr B.P. the ocean reservoir correction is approximately $400 \pm$ yr, thus somewhat less than the correction derived from sites to the east of 326PC for Preboreal times (Hafliðason et al., 2000). However, we apply a 400-yr correction to our dates (Table 1), and it is these corrected ages that we report in the text. Dates in kilo years (ka B.P.) are rounded to the nearest decimal point. The 400-yr correction is probably a minimum estimate for MIS2 and 3 (Voelker et al., 1998; Hagen, 1999).

Radiocarbon dates (Table 1) from within the diamictons give ages of >25 ka B.P. (Figs. 4 and 5). The uncorrected date of 9120 ± 130 yr B.P. in the middle of 322PC is far too young—it was based on a very small sample. The dates near the base of the fined-grained lithofacies in 323PC and 326PC range between ~ 12.7 and $13.4 \pm$ ka B.P. (Figs. 4 and 5). In 322PC the date at the transition is $11.57 \pm$ ka B.P., but the entire postglacial section in this core is only 30 cm or so; hence a date from a 2-cm interval can be only an estimate because we expect contamination from bioturbation. The dates immediately above the diamictons indicate that the net sediment accumulation rate (cm/ky) was extremely low, especially considering typical depositional rates of hundreds of centimeters per kiloyear during ice retreat off glaciated shelves (Andrews and Syvitski, 1994; Hafliðason et al., 1998), and when compared with deglacial accumulation rates values off southwest Iceland (Syvitski et al., 1999; Jennings et al., 2000).

The seismic data along the track to 326PC suggested (Fig. 3) sediment loss above the Saksunarvatn reflector, and the radiocarbon dates confirmed this (Fig. 5). For example, the date above the tephra

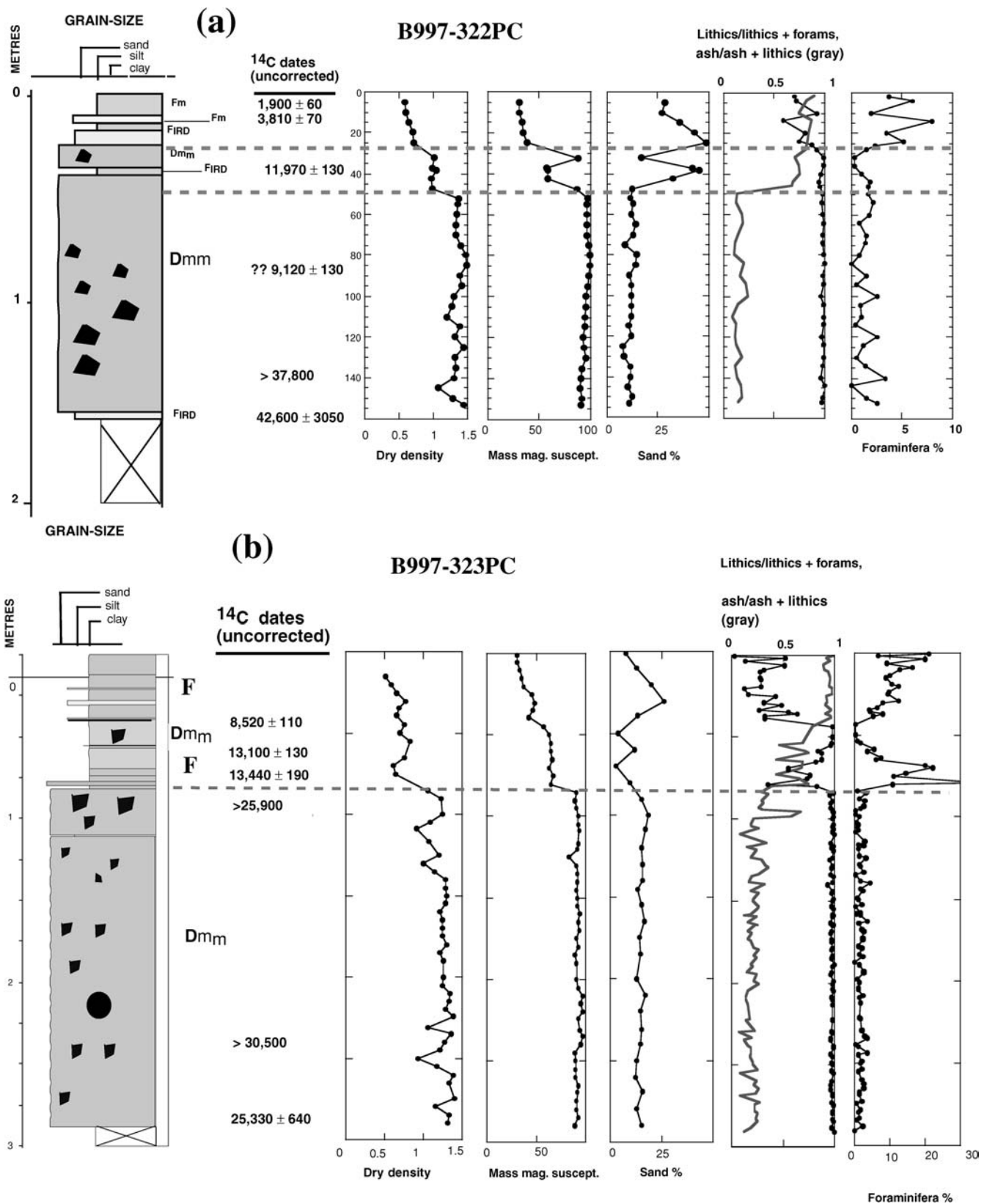


FIGURE 4. (a) Lithofacies (*Dmm* = massive matrix supported diamictos, *F* = fine-grained), radiocarbon dates, and sediment properties of B997-322PC. Gray horizontal lines indicate breaks in properties (see text). Units for density are g/cc and for mass magnetic susceptibility they are $\times 10^{-7} \text{ m}^3/\text{kg}$. The fourth column shows sediment composition as: lithics/lithics + forams as the black line with filled circles, and the ratio of ash/ash + lithics as the solid line. (b) Lithofacies and properties for B997-323PC. Gray horizontal lines indicate breaks in properties (see text). Radiocarbon dates and errors are shown. Units for density are g/cc. The fourth column shows sediment composition as: lithics/lithics + forams as the black line with filled circles, and the ratio of ash/ash + lithics as the solid line.

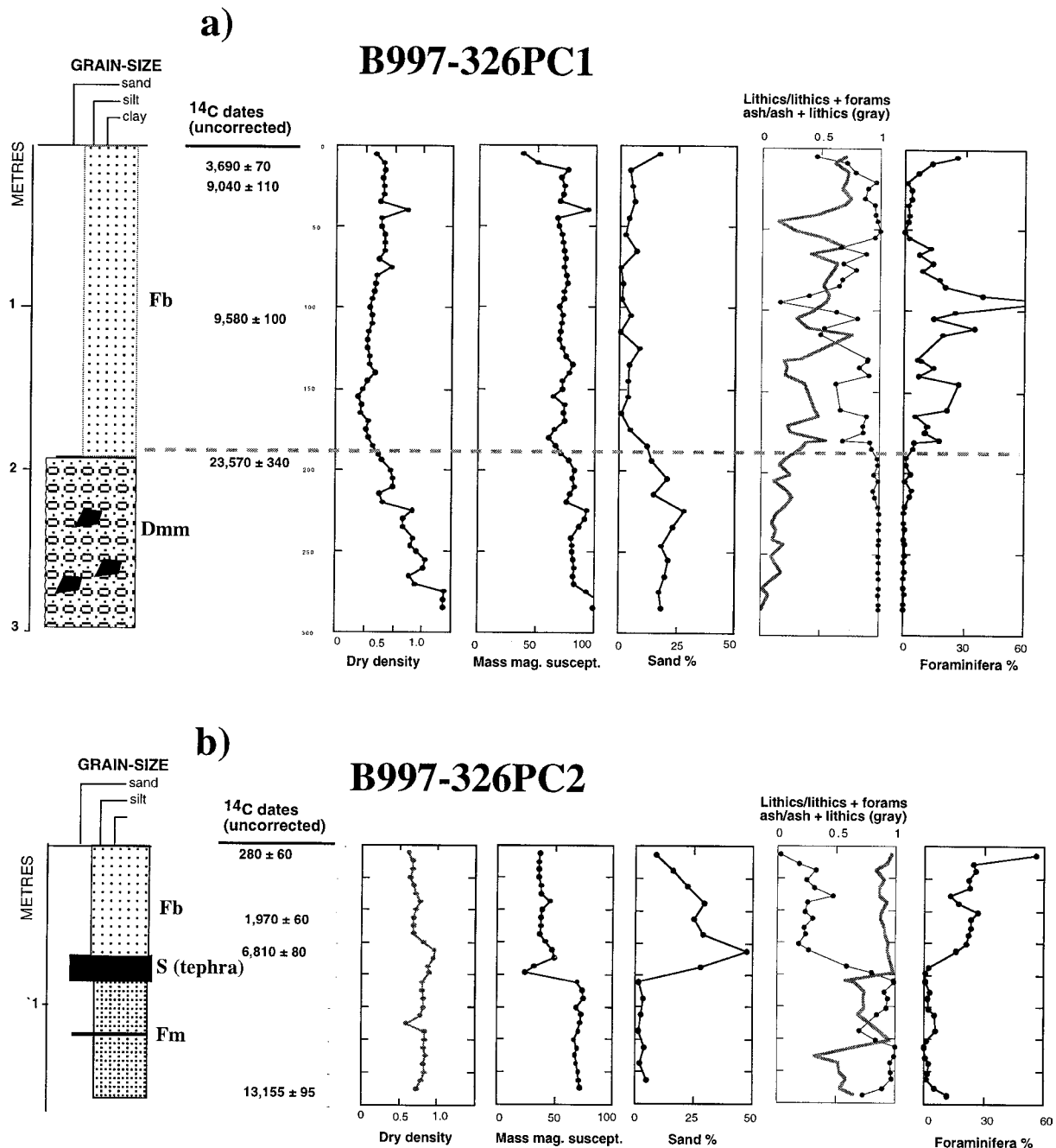


FIGURE 5. (a) Lithofacies and properties B997-326PC1. Gray horizontal lines indicate breaks in properties (see text). Radiocarbon dates and errors are shown. Units for density are g/cc and for mass magnetic susceptibility they are $\ast 10^{-7} m^3/kg$. The fourth column shows sediment composition as: lithics/lithics + forams as the black line with filled circles, and the ratio of ash/ash + lithics as the gray line. (b): Lithofacies and properties B997-326PC2. Radiocarbon dates and errors are shown. Units for density are g/cc . The fourth column shows sediment composition as: lithics/lithics + forams as the black line with filled circles, and the ratio of ash/ash + lithics as the gray line.

unit in 326PC2 is only 6.4 ± 0.08 ka B.P., and within a few centimeters of this date is an age of 1.57 ± 0.06 ka B.P. Similarly, at 326PC1, dates of ~ 8.6 and 3.3 ka B.P. were obtained within a few centimeters of each other (Table 1).

TEPHRAS IN THE CORES

Our concern in this section is to ascertain whether we can correlate peaks in the tephra counts (e.g., Figs. 4 and 5). Little change in the occurrence of tephra is noted in the counts from the diamicton

units in our cores, but there are decided changes within the fine-grained facies. Volcanic activity occurred both during deglaciation and postglacial times (Sjoholm et al., 1991; Bjorck et al., 1992; Hardardóttir, 1999; Geirsdóttir et al., 2000; Hardardóttir et al., 2001; Bond et al., 2001). Even during the LGM, volcanic eruptions probably spread ash onto the ice sheet, just as happens today (Larsen, 2000). Jennings et al. (2002) reported finding tephra associated with Ash Zone II (~ 50 ka B.P.) in deglacial (12 ka B.P.) sediments off East Greenland indicating that care must be exercised in differentiating between a primary ash-fall unit and ash peaks resulting from the release of glacially stored tephra.

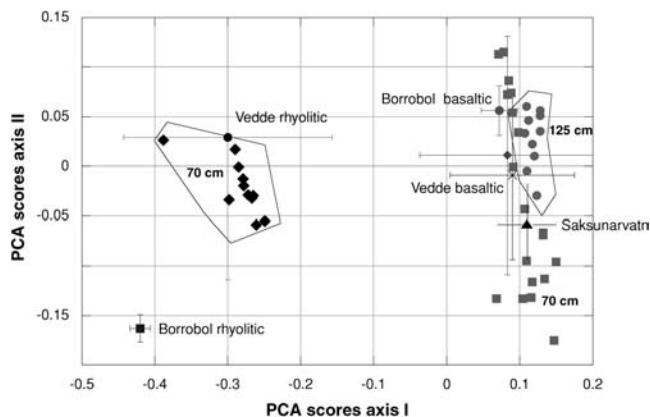


FIGURE 6. Results of Principal Component analysis of logratio data on major elements from known tephra and samples from cores 322, 323, and 326 (see Fig. 10). The example here shows plots on the 1st two PC axes of samples from 326PC2 from depths of 70 and 125 cm against the average for basaltic (bas) and rhyolitic (rhy) for widespread regional tephra (see text).

We used a total of 149 individual analyses, of which 69 were from known regional tephra, including data from the Vedde and Saksunarvatn tephra in core MD99-2269 in Húnaflóaáll (Grönvold, personal communication 2000). The HM107-05 data were used as a local representative of the Borrobol tephra (Turney et al., 1997) with an associated date of $13,700 \pm 140$ B.P. (Fig. 7 of Eiriksson et al., 2000a). In the Greenland Ice Sheet, the Vedde and Saksunarvatn tephra have sidereal ages of $11,980 \pm 80$ and $10,180 \pm 60$ cal yr respectively (Grönvold et al., 1995), and radiocarbon dates on terrestrial and marine sediments of $10,300 \pm$ and $9000 \pm$, respectively (Birks et al., 1996; Wastegard et al., 1998; Wastl et al., 1999).

Geochemical data are often presented as biplots of two elements or the ratios of elements. We employ a multivariate approach based on taking log ratios of the data (because the elements sum to 100%, hence are not independent estimates, Aitchison, 1986; Reyment and Savazzi, 1999). We use Principal Component Analysis (PCA) (Kovach, 1998) to assign unknown tephra to Borrobol, or Vedde, or Saksunarvatn, or to recognize a “mismatch.” On Figure 6 we illustrate our graphical approach; we plot the mean PCA scores and standard deviations for known tephra on the two PCA axes and compare these with two “unknown” tephra from 326PC2. The two axes explain 84% of the geochemical variability; 64% is explained by the first axis alone. The first axis is associated with SiO_2 (−0.382), Al_2O_3 (−0.343), MgO (0.388) and CaO (0.365). The second axis is associated most strongly with MnO (0.523) and K_2O (−0.487). If the data are log ratio transformed but not standardized, the first two PCAs explain 92.5% of the variance. The correlation between the PCA loadings on these two solutions (standardized and not standardized) is $r = 0.79$, indicating that both approaches capture much the same information. For each site we plotted the PCA scores for the unknown tephra. Because there is such a marked distinction between the silica-rich rhyolitic shards and the more basaltic fraction, we also ran the PCA analysis of a reduced data set of only basaltic shards. This analysis produced two PCAs that explained 79% of the variance (PCA1 = 65%). The first PCA was most strongly positively loaded on SiO_2 and CaO , with negative loadings on K_2O and P_2O_5 . The second axis was dominated by Na_2O (positive) and FeO^* .

Table 2 lists limiting radiocarbon dates and possible geochemical affiliations based on these data, and in Figure 7 we suggest correlations based on the geochemical PCA data and available radiocarbon dates (Table 1). We view these correlations as reasonable and testable hypotheses. Our method does not always provide a single best fit. For

TABLE 2

Limiting radiocarbon dates and possible correlative tephra based on the geochemistry of the samples (see Fig. 7)

Site and depth (cm)	Limiting dates (estimates)	Ash correlation
B997-326PC2		
68–80	$\sim 6,400 \pm$	Vedde and Saksunarvatn—reworked
125	$>6,400$ & $<12,700$	Vedde/Borrobol? basaltic
150	$\sim 12,700 \pm$?
B997-326PC1		
75	$<9,180 \pm$?
115	$\sim 9,180 \pm$	Saksunarvatn?
B997-323PC		
30	$<8,100 \pm$	Vedde—reworked?
68	$12,700 \pm$	Borrobol?
94	$>25,500$?
B997-322PC		
25	$>3,400$ and $<11,570$	Vedde?
48	$>11,570$	Borrobol?

example, the individual grains from 326PC2 at 68–80 cm have geochemical affinities with both the Vedde and Saksunarvatn tephra. Given the seismic stratigraphy at this site (Fig. 3), the radiocarbon date from within the unit (Table 1), and the PCA scores (Fig. 6), we conclude that this interval represents reworking of two primary ash-fall tephra. The tephra at 125 cm in this core appears to have a reasonable correlation with the Vedde/Skogar ash (Norrdahl and Hafidason, 1992) (Fig. 7), and this correlation is not disputed by the bracketing radiocarbon dates. The tephra at the base of 326PC2 is possibly coeval with ash deposition in HM107-05, to the east of our site.

Core Stratigraphy and Composition

The principal lithofacies we identified included massive matrix-supported diamictos, bioturbated or massive muds, mud with iceberg-rafted detritus, and sand (Figs. 4, 5). Very sharp contacts between diamictos and overlying sediments occurred in cores 322PC, 323PC, and 326PC1. We present data on sediment and foraminiferal properties and then evaluate the origins and environments of deposition.

B997-322PC: The lowermost unit is a diamicton (Fig. 8) with a dry density of 1.33 ± 0.12 g/cm³, although there is a hint from the X-radiography that this facies terminates above the base of the core (Fig. 4A). The major break in physical properties occurs at 50 cm, although another distinct change occurs at ~ 38 cm. Within the upper 50 cm are several lithofacies changes including the occurrence of another diamicton. At 50 cm there is an abrupt decrease in dry sediment density and mass magnetic susceptibility (mass MS), whereas sand percentage increases. The ratio of ash:ash+lithics changes abruptly at 50 cm from ~ 0.2 to 0.7, denoting a significant increase in the contribution of volcanic shards. This change is also associated with a decrease in clasts >2 mm (not shown). Dark basaltic glass rises first at 48 cm, but there is a distinct peak in clear, rhyolitic glass shards at 25 cm (Fig. 7). Total carbonate, a measure of marine productivity, remains at ca. 1.5% for much of the core, with a decrease in the upper diamicton, before rising rapidly to values of 3–4%. This pattern is paralleled by the percentages of foraminifera, with a distinct barren zone between 30 and 40 cm.

Thus the overall summary for this core is that conditions were relatively stable from near the base of the core to ca. 50 cm, when the environment changed considerably, as reflected in the physical properties within the uppermost 50 cm (Table 2). The ¹⁴C dates and

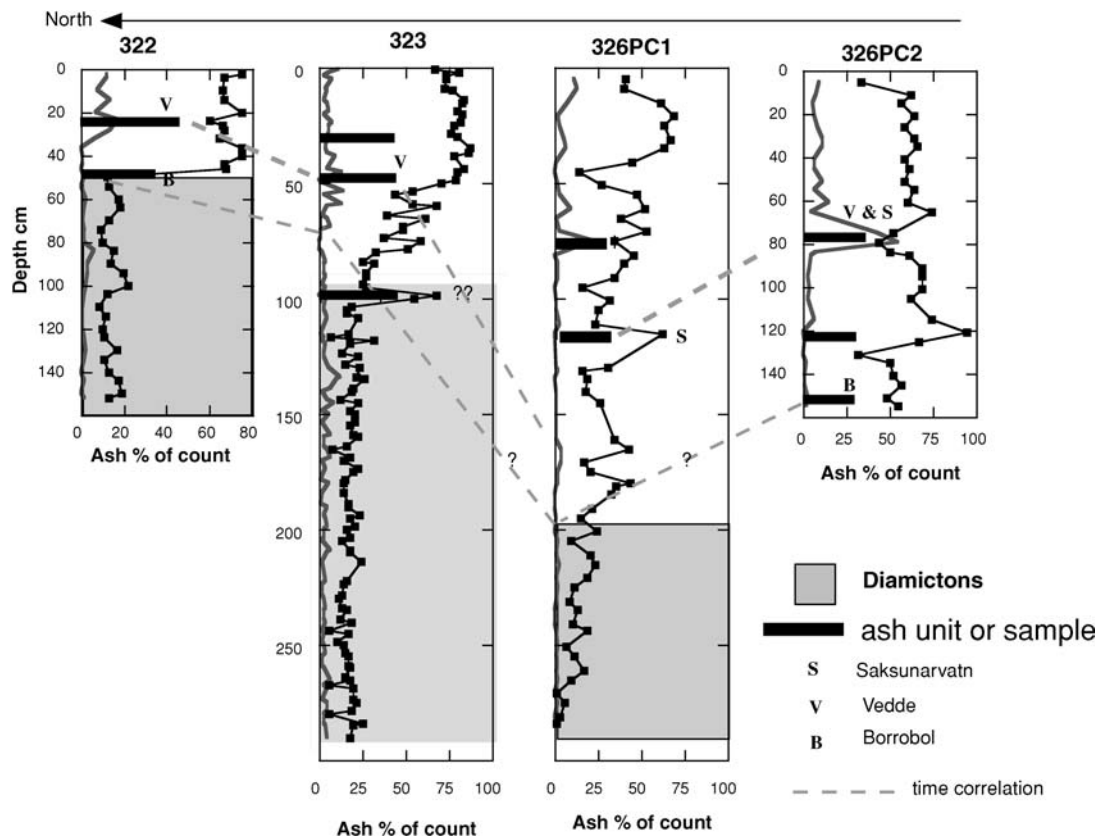


FIGURE 7. Plots of tephra (black line = basaltic; gray line = rhyolitic) as a percentage of the total sediment count in the $>105 \mu\text{m}$ sand fraction, and possible correlations between tephra in these cores with the three most widespread regional tephra deposited between ca. 9 and 13 ka B.P. The correlations (gray dashed lines) are based on geochemistry and bracketing radiocarbon dates.

tephra correlations (Figs. 4, 7) indicate that the diamictons are associated with dates 25 ka B.P. and that the transition to a thin, postglacial unit dates from 11.6 ka B.P.

B997-323PC: The sediments consists of over 2 m of diamicton (Fig. 8) overlain by a complex of lithofacies (Fig. 4B). The contact is sharp and occurs at 80 cm. Within the diamicton, sediment density averages $1.23 \pm 0.12 \text{ g/cm}^3$. The change in lithofacies at 80 cm is well seen in the density log and in the mass MS values (Fig. 4B and Table 3); however, the carbonate and total organic carbon data change closer to 40 cm (not shown), at the contact with a thin diamicton characterized by large clasts. The numbers of iceberg-rafted clasts are generally >20 although there are intervals with little evidence for such at 225, 80, and over the last 20 cm. Both the lithic and ash ratios show the major change at 80 cm (Fig. 4B), indicating that this change in lithofacies represents the major transition in the environments of deposition. Foraminifera were noted in small but consistent numbers throughout the lower diamicton but rise abruptly at 80 cm only to decrease to 0% at 40–50 cm before rising again. There is no obvious signal in the sand, which averages about 15%. Dates from within the lower diamicton give ages 25 ka B.P. whereas the overlying muds are 13 ka B.P. There is thus a temporal hiatus of ~ 12 ky in the late Quaternary stratigraphic sequences in cores 322PC and 323PC.

B997-326PC1 and PC2: Cores 322PC and 323PC lie in Húnaflóadjúp, about equidistant from Húnaflói and the Strandir coast (Figs. 1, 2). Cores 326PC1 and 326PC2, however, lie in Reykjafjarðaáll (Fig. 2).

Core 326PC1 has a diamicton in the lowermost meter of the core (James, 1999) (Fig. 5A). Dry sediment density averages $1.31 \pm 35 \text{ g/cm}^2$, although it decreases steadily from the base of the core to the

main lithofacies boundary at 195 cm. Mass MS shows no obvious decrease across this boundary, in contrast with 322PC and 323PC (Fig. 4A, B), but sand percentages do decrease in the muddy facies probably owing to an increase in airborne tephra (Table 3). The Saksunarvatn tephra is tentatively located at ~ 120 cm (Fig. 7). The percentage of foraminifera in the $>105\text{-}\mu\text{m}$ fraction increase from extremely low values (frequently barren) in the diamicton facies to between 20–30% in the middle section of the overlying muddy facies. The boundary between these two lithofacies is also evident in the lithics:total and ash:ash+lithics ratio graphs (Fig. 5A), which supports the argument that a major environmental change occurred at this transition. Dates above and below the facies boundary replicate the data from 322PC and 323PC (Fig. 4) and define a significant late Quaternary 12-ky depositional hiatus.

Core 326PC2 is predominantly fine-grained mud with various amounts of iceberg-rafted clasts. There is a distinct 10-cm-thick tephra unit at 70 cm which has a mixed composition (Fig. 7). The sediment above the ash has no visible iceberg-rafted component on the core X-radiographs. The radiocarbon dates and tephra stratigraphy (Figs. 5, 7) indicate limited deposition with some erosion and reworking over the last ~ 12.7 ka B.P.

SUMMARY AND THE STRATIGRAPHIC PROBLEM

Table 3 summarizes the average differences between the two principal lithofacies at our core sites. An in-depth analysis of the diamictons in these cores using a variety of micro- to macrofabric techniques is in progress (e.g., Principato, 2000, 2003). The <2 mm grain-size spectra of the diamicton facies (Fig. 8) show distinct tails

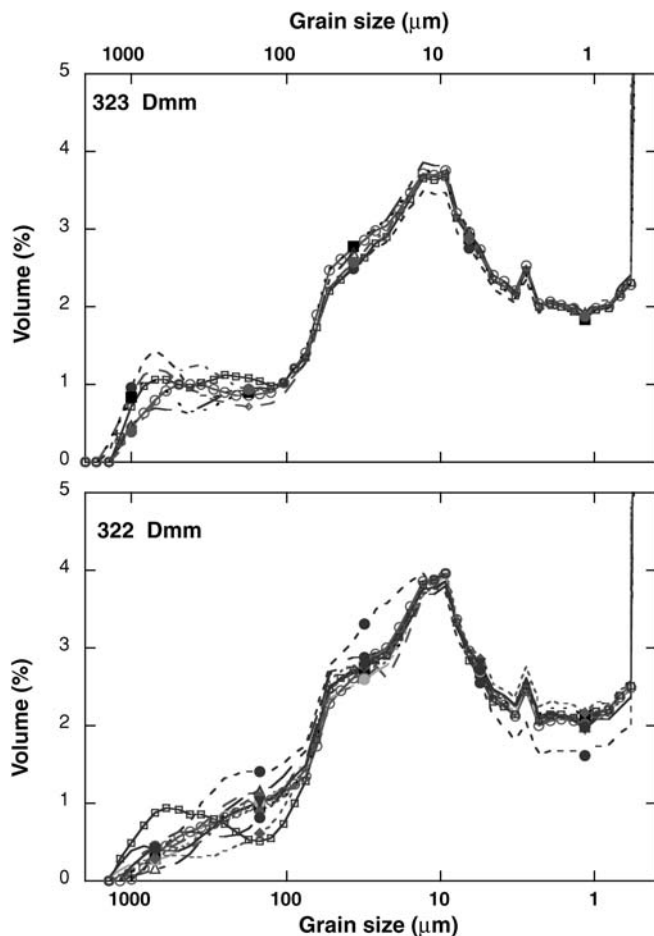


FIGURE 8. Grain-size spectra of the diamictons (Dmm) in the < 2000- μm fraction in cores B997-323PC and 322PC. The various line-types represent individual samples; notice how similar the grain size spectra are both within each diamicton and between the two sites.

in both the very coarse sand and the very fine clay (<0.49 μm). However, in all the diamictons the modal grain size is $\sim 10 \mu\text{m}$, with subsidiary modes in the sand fraction (Andrews and Principato, 2002). Composition counts of the >105 μm fraction indicate that “foreign” lithics (e.g., quartz) are also present in the postglacial sediments, suggesting some transport of materials to the shelf from sea ice or iceberg rafting (Eiriksson et al., 2000a, 2000b), or from the reworking of older Quaternary sediments. Angular basaltic and rhyolitic shards make up a substantial fraction of the sand-size sediment. Visible tephra layers were evident only in 326PC2 (Fig. 5B), but major peaks in ash content may represent discrete volcanic ash falls (Fig. 7).

The succession of diamictons (pebbly muds) overlain by fine-grained marine muds is a common deglacial/postglacial succession around most glaciated continental margins (e.g., Jennings, 1993). In these cases, radiocarbon dates from the diamictons date from initial deglaciation of the shelf. The transition to sediments devoid of iceberg rafted clasts reflects the final deglaciation of the shelf and the location of the ice margin on land. Thus, ^{14}C dates from these successions result in conformable depth/age plots. However, in the case of 322PC, 323PC, and 326PC1 this is not the case; rather there is a 12 ky hiatus between deposition of the diamictons and the overlying mud (Figs. 4, 5). The 12 ky gap in the sedimentary record can represent nondeposition or loss by erosion, and the interpretation of this hiatus lies at the heart of deciphering the extent of ice at the LGM.

TABLE 3

Comparison of average sediment properties between the diamictons and the fine-grained mud facies (see Figs. 4 and 5) (B997-322PC, -323PC, -326PC1 and -326PC2, respectively)

Property	Fine-grained lithofacies (F)	Diamicton Facies (Dmm)
Dry density (g/cm^3)	0.82, 0.68, 0.67, 0.77	1.28, 1.22, 1.28, N/A
Mass mag. suscept. ($\times 10^7 \text{ m}^3/\text{kg}$)	51.2, 50.8, 70.7, 53.6	94.9, 91.6, 84.8, N/A
Sand %	33.2, 12, 4.8, 15.0	11.5, 15, 19.5, N/A
Lithics/lithics + forams	0.86, 0.54, 0.77, 0.61	0.98, 0.98, 0.98, N/A
Ash/ash + lithics	0.74, 0.79, 0.47, 0.78	0.16, 0.22, 0.13, N/A
Foram %	2.7, 9.8, 13.8, 12.0	1.3, 1.7, 0.8, N/A

N/A = Not applicable.

Foraminifera and Stable Isotopes: Cores 322PC and 323PC

Our work on the foraminifera was designed to contribute information on the origins of the sparse but pervasive foraminifera in the diamictons in 322PC and 323PC and to evaluate the environment during deglaciation. Foraminifera are present in 326PC and 326PC2 (see Fig. 5A and 5B), but species identifications have not been carried out. Four main biofacies have been delimited and are discussed further below and identified as 322PC-a, 323PC-A, etc (Fig. 9).

The presence of macro- and microfossils is a key element in debates over glacial versus glacial-marine origins of shelf diamictons (Dreimanis, 1979; Andrews and Matsch, 1983; Licht et al., 1999). Neither 322PC nor 323PC has sufficient sediment thickness for us to extract a high-resolution record of events since deglaciation 13 ka B.P.

The results of the foraminifera identification (Fig. 9A and 9B) confirm the presence of low but persistent numbers of benthic foraminifera within the diamictons, with values ranging in the few hundred individuals per 100 g. Faunal zones 322PC-a and 323PC-A are dominated by *Cassidulina reniforme*, *Elphidium excavatum*, and *Islandiella norcrossi*. Also present in reasonable percentages are *Cassidulina neoteretis* and *Cibicides lobatulus*. This assemblage has similarities with the present benthic faunas from Djúpall (Fig. 1) (Jennings et al., in press) and from the East Greenland shelf 66–68°N (Jennings and Helgadóttir, 1994; Jennings and Weiner, 1996). Perhaps of most interest is the presence of *C. neoteretis* which today is linked with the presence of modified Atlantic Water.

The numbers of planktonic foraminifera per 100 g of sediment was very low within the diamicton facies, but sufficient numbers (~ 20) were extracted for isotopic analyses (Fig. 10). The results from both 322PC and 323PC indicated that the surface waters were either quite fresh or that deposition occurred during an interval of moderate water temperatures. The $\delta^{18}\text{O}$ indicate values of 3.8‰ to 3.0‰ in 322PC and between 3.5‰ and 2.5‰ in 323PC. Samples of *N. pachyderma* s from the present sediment/water interface at these two sites gave $\delta^{18}\text{O}$ values of 2.79‰ and 2.38‰, respectively, indicating that near-surface waters were enriched (more glacial) in ^{18}O during deposition of biofacies a and A (Fig. 9A, 9B). The $\delta^{18}\text{O}$ values in 322PC and 323PC, facies a and A (Fig. 10), are similar to core-top ratios on planktonic foraminifera from the East Greenland margin between 66° and 68°N (Smith, 2001) and are generally lighter than MIS2 and MIS3 $\delta^{18}\text{O}$ values from Blossville Basin, north of the Denmark Strait (Hagen, 1999; Voelker, 1999).

At the transition from massive diamictons to a fine-grained, iceberg-rafted debris (Figs. 4, 9) there is a rapid increase in the numbers of both benthic and planktonic foraminifera (facies b and B). In 323PC the transition is marked by spikes in three of the four major species and the sudden appearance of *Alabaminiella weddellensis*,

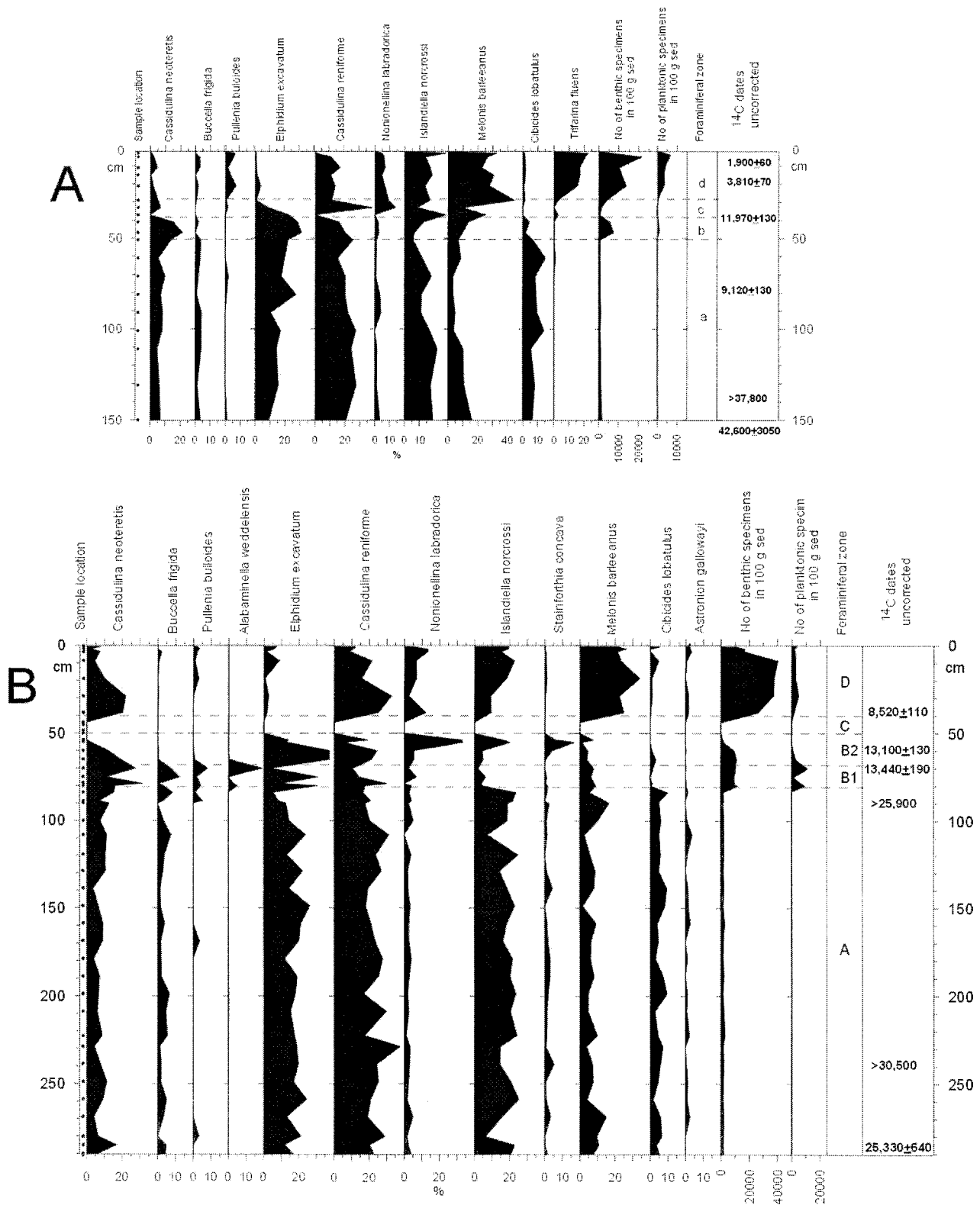


FIGURE 9. (a) Foraminifera nos/100 gr and main species (% data) for B997-322PC and (b) 323PC. Radiocarbon dates are listed in the last column with the biozone breaks in the adjacent column.

which might indicate an increase in phytodetritus (Jennings, personal communication, 2002). However, there is no marked change in $\delta^{18}\text{O}$ values (Fig. 10). There is a marked reduction in numbers of foraminifera in biofacies 322PC-c and 323PC-C; this interval is essentially a “barren zone” marked by an increase in iceberg-rafted accumulation (Fig. 4A, 4B). However, sufficient planktonic forami-

nifera were picked to record a sharp increase in $\delta^{18}\text{O}$ to the largest values in either core, with $\delta^{18}\text{O}$ values between 3.5‰ and 4‰ (Fig. 10). Based on the stratigraphy and bounding radiocarbon dates (Fig. 4) this cold, clast-rich interval coincides with all or part of the Younger Dryas cold interval (Ruddiman and McIntyre, 1981). East of our study area in cores HM107-04 and -05, the data of Eiriksson et al.’s (2000a,

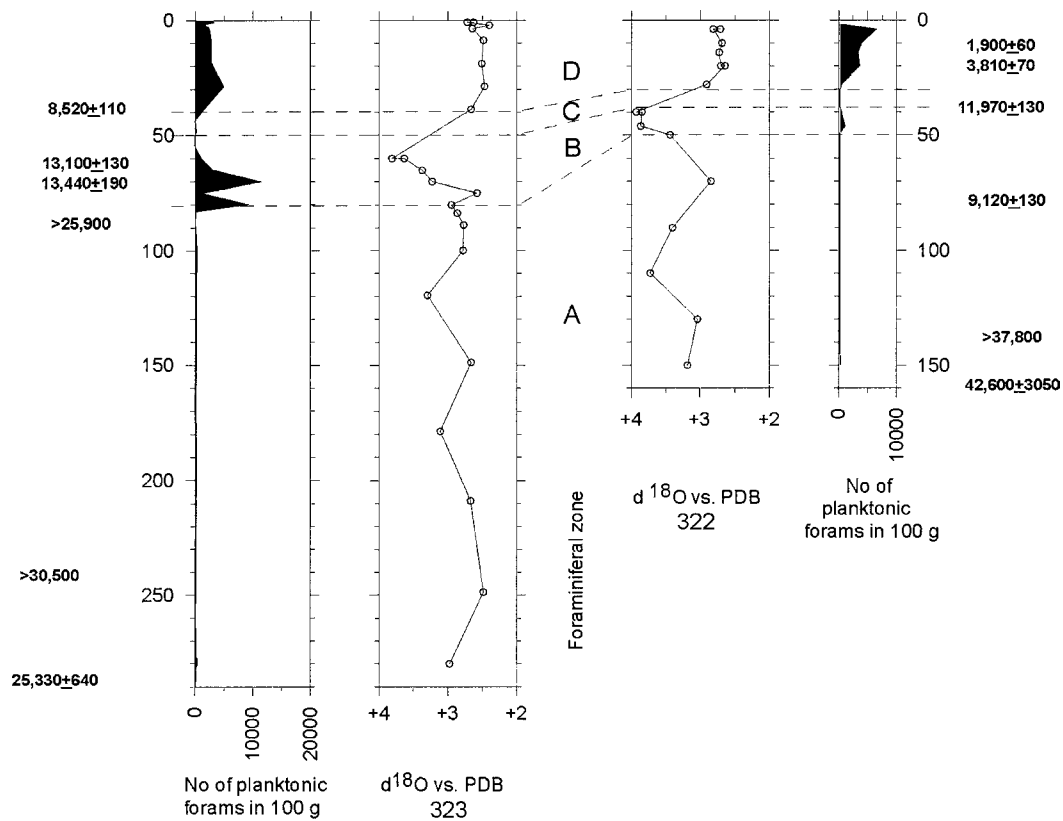


FIGURE 10. (a) Numbers of planktonic foraminifera and stable $\delta^{18}\text{O}$ values for B997-323PC and (b) B997-322PC. Note the “barren zone” in both cores near the 50 cm depth mark. The dashed lines delimit the faunal boundaries identified in Figure 9 and show the inferred correlations on the foraminiferal zonation.

their Figs 8, 10) also show an interval with virtually no foraminifera at approximately the same time.

The last 10 ka B.P. are represented in these two cores by only ~40 cm of sediment, whereas to the south of these sites the Húnaflóaíall sediment body (Fig. 3, core MD99-2269) reaches a thickness of 25 m over the same interval of time owing to sediment focusing (Andrews et al., 2002a). Numbers of foraminifera rise rapidly in both cores, although both also indicate a noticeable decrease in numbers in the top few centimeters (Fig. 9A, 9B). A notable feature of the Holocene is the reduced contribution of *E. excavatum* to the assemblages and the increase in *Melonis barleeanus*. At other sites on the north Iceland shelf, *E. excavatum* was reintroduced into the fauna in the last 1–2 ka B.P. (Eiriksson et al., 2000a; Andrews et al., 2001). The $\delta^{18}\text{O}$ data have consistent values of between 2.5‰ and 2.8‰ (in facies d and D, Fig. 10).

The foraminifera and $\delta^{18}\text{O}$ data indicate that the diamictites in 322PC and 323PC have consistent assemblages and isotopic ratios. The data do not show a “mixed” fauna, as has been noted in some glacial-marine/glacial settings caused by glacial reworking (Jennings et al., 1998); individual tests showed little evidence of crushing. The major distinction between the diamictites and the overlying “post-glacial” sediments is in the number of foraminifera per 100 g of sediment (Fig. 9)—this transition occurs at the main lithofacies boundary in both cores.

Discussion and Conclusions

Quaternary sediments in Húnaflóadjúp consist of a basal diamictite overlain by a Holocene “drift-like” sediment body that reaches a maximum thickness of 25–30 m between 323PC and 326 (Fig. 3C) (Andrews et al., 2002a). Our sites (Fig. 2) are at the northern

(322PC, 323PC) and southern (326PC) limits of the shelf sediment drift. At these sites the diamictite is overlain by only 30–200 cm of glacial-marine and marine sediments (Fig. 3A, B).

How we map the LGM extent of glacial ice onto the north Iceland shelf, off the Northwest Peninsula, clearly depends on how we interpret the origin of the diamictites in cores 322PC, 323PC, and 326PC (Figs. 4, 5). Similarly, estimates of the dates of deglaciation depend on the interpretation of the environments of deposition at the major lithofacies transition in these same cores. Radiocarbon dates at the base of the fine-grained facies are 12.5–13 ka B.P., whereas dates within the diamictites facies are 25 ka B.P. A critical question is how do we explain the 12-ky gap between the dates in the diamictites and those in the overlying fine-grained muds?

The diamictites at the three sites have similar properties (Table 3) and are distinct from the fine-grained lithofacies. There is a small but pervasive presence of foraminifera in cores 322PC and 323PC, whereas the base of 326PC1 is virtually barren (Fig. 5A). The key issue that pertains to the extent of glacial ice in the field area (Fig. 2) is whether the diamictites in 322PC, 323PC and 326PC1 (Figs. 4, 5) represent (1) basal tills; (2) glacially reworked glacial-marine sediments, possibly remolded as a deforming bed (Cofaigh and Evans, 2001); or (3) *in situ* glacial-marine sediments. Detailed investigations of the diamictites are in progress to better understand their depositional history (Principato, 2000). If the diamictites are tills or glacially reworked sediments, then the limit of glaciation is seaward of a core site, whereas if the sediments represent glacial-marine deposition, then the glacial margin must have lain landward. The persistent, if limited, presence of intact foraminifera in 322PC and 323PC (Fig. 9) suggests that either option 2 or 3 applies to these outer sites, whereas the lack of foraminifera in 326PC1 may indicate an origin more associated with subglacial deposition, hence probably option 1. The first two scenarios

would place the limit of the LGM glaciation close to the north Iceland shelf break beyond 322PC, whereas option 3 would draw the LGM grounding line somewhere between 326PC and 323PC. The dry density data from the diamictos (Table 3) does not indicate substantial compaction; indeed, they are substantially lower than values from glacial-marine sediments in the Puget Lowlands, where densities ranged between 1.62 and 2.2 g/cm³ (Easterbrook, 1964). Data from a wide range of glacial-marine sediments on the northeast Canadian margin gave wet sediment densities of between 1.65 and 2.1 g/cm³ for ice-proximal glacial-marine sediments (Andrews et al., 1991), which compares favorably to data from the diamictos in 322PC, 323PC, and 326PC1 of between 1.6 and 2.0 g/cm³.

However, an in situ glacial-marine origin for the diamictos poses chronological and depositional problems. For example, why are there no sediments >13 and <25 ka B.P.? We suggest that the application of “Occam’s razor” leads to the conclusion that the stratigraphy and chronology at 322PC and 323PC are best explained by glacial ice overrunning the sites and remolding glacial-marine sediments deposited 25 ka. The ice cap persisted in Húnaflóadjup from sometime after 25 ka until ~13 ka. Given the evidence for a restricted ice cap on the Northwest Peninsula, with an ice stream only extending a little way beyond the mouth of Isafjordardjup (Fig. 1) (Andrews et al., 2002c; Geirsdóttir et al., 2002d), then our conclusion requires an extensive ice stream in Húnaflóaál/Húnaflóadjup fed by ice accumulating in the highlands of west-central Iceland, possibly centered on the Langjökull massive (Bourgeois et al., 2000).

Regardless of the origin(s) of the diamictos, a major puzzle is why deposition during deglaciation (ca. 9–13 ka B.P.) was so limited (Figs. 3, 4, and 5)—this is unusual, especially when compared to the considerable thicknesses of glacial-marine sediments on the formerly glaciated continental margins of northeast Canada (Piper et al., 1991; Andrews, 2000), East Greenland (Dowdeswell et al., 1994), Norway (Vorren et al., 1983), and SW Iceland (Syvitski et al., 1999; Jennings et al., 2000). The most probable explanation for the limited thickness of glacial-marine sediments on the north Iceland shelf is that the ice margin retreated very rapidly across the shelf, giving limited time for sediment accumulation. The ice-rafted, clast-rich interval and foraminiferal barren zone in 323PC suggests a return to glacial-marine conditions during the Younger Dryas cold event. The regional interpretation of the strong Younger Dryas signal (Fig. 4) awaits integration into the evaluation of ice-rafted sediments from sites to the west (Geirsdóttir et al., 2002) and east (Kristjansdóttir, 1999; Eiriksson et al., 2000a) of our area.

Acknowledgments

We thank the Marine Research Institute, Iceland, for its support in terms of ship time in 1997. The data were collected with support from the National Science Foundation (ATM-9531397, OPP-972510, and OCE98-09001) and the Marine Research Institute. We thank Rolf Kihl for providing the sedimentological analyses and Rindy Osterman (Woods Hole Oceanographic Institute) for her assistance in the stable isotope laboratory. The paper has been read by Dr. Anne Jennings and Sarah Principato. We appreciate the reviews of Drs. Aslaug Geirsdóttir and C. Caseldine who greatly assisted in the preparation of the present version of the manuscript. The data will be made available on www.ngdc.noaa.gov/paleo/parcs/mapsearch.html.

References Cited

Aitchison, J., 1986: *The Statistical Analysis of Compositional Data*. London: Chapman and Hall. 416 pp.
 Andrews, J. T., 2000: Rates of marine sediment accumulation at the margin of the Laurentide Ice Sheet 14 ka B.P. *Journal Sedimentary Research*, 70: 782–787.

Andrews, J. T., in press: A review: Late Quaternary marine sediment studies of the Iceland shelf, Paleooceanography and land/ice sheet/ocean interactions. In: Caseldine, C. (ed.), *The Environments of Iceland*. Amsterdam: Elsevier.
 Andrews, J. T. and Matsch, C. L., 1983: *Glacial-Marine Sediments and Sedimentation: An Annotated Bibliography*. Norwich, U.K.: Geo Abstracts Ltd. 227 pp.
 Andrews, J. T., and Principato, S. M., 2002: Grain-size characteristics and provenance of ice-proximal glacial marine sediments (or why do grain-size analyses anyway?). In Dowdeswell, J. A. and O’Cofaigh, C. (eds.), *Glacier-influenced Sedimentation at High-Latitude Continental Margins*: Geological Society of London, Special Publication 203, 305–324.
 Andrews, J. T., and Syvitski, J. P. M., 1994: Sediment fluxes along high latitude continental margins (NE Canada and E Greenland). In Hay, W. (ed.), *Material Fluxes on the Surface of the Earth*. Washington, D.C.: National Academy Press, 99–115.
 Andrews, J. T., Jennings, A. E., MacLean, B., Mudie, P., Praeg, D., and Vilks, G., 1991: The surficial geology of Canadian eastern Arctic and Polar continental shelves. *Continental Shelf Research*, 11: 791–819.
 Andrews, J. T., Smith, L. M., Preston, R., Cooper, T., and Jennings, A. E., 1997: Spatial and temporal patterns of iceberg rafting (IRD) along the East Greenland margin, ca. 68 N, over the last 14 cal ka B.P. *Journal of Quaternary Science*, 12: 1–13.
 Andrews, J. T., Hardardóttir, J., Helgadóttir, G., Jennings, A. E., Geirsdóttir, A., Sveinbjornsdóttir, A. E., Schoolfield, S., Kristjansdóttir, G. B., Smith, L. M., Thors, K., and Syvitski, J. P. M., 2000: The N and W Iceland shelf: insights into Last Glacial Maximum ice extent and deglaciation based on acoustic stratigraphy and basal radiocarbon AMS dates. *Quaternary Science Reviews*, 19: 619–631.
 Andrews, J. T., Caseldine, C., Weiner, N. J., and Hatton, J., 2001: Late Quaternary (~4 ka B.P.) marine and terrestrial environmental change in Reykjarfjörður, N. Iceland: climate and/or settlement? *Journal Quaternary Sciences*, 16: 133–144.
 Andrews, J. T., Hardardóttir, J., Kristjansdóttir, G. B., Grönvold, K., and Stoner, J., 2002a: A very high resolution sediment record from Hunafloall: Holocene century-scale variability along the N Iceland margin. *The 25th Nordic Geological Winter Meeting*, abstract volume: 10.
 Andrews, J. T., Kihl, R., Kristjansdóttir, G. B., Smith, L. M., Helgadóttir, G., Geirsdóttir, Á., and Jennings, A. E., 2002b: Holocene sediment properties of the East Greenland and Iceland continental shelves bordering Denmark Strait (64°–68°N), North Atlantic. *Sedimentology*, 49: 5–24.
 Andrews, J. T., Hardardóttir, J., Geirsdóttir, A., and Helgadóttir, G., 2002c: Late Quaternary ice extent and depositional history from the Djúpáll trough, Northwest Peninsula, Iceland: a stacked 36 cal ka environmental record. *Polar Research*.
 Andrews, J. T., Geirsdóttir, A., Hardardóttir, J., Principato, S., Kristjansdóttir, G. B., Helgadóttir, G., Grönvold, K., Drexler, J., and Sveinbjornsdóttir, A., 2002d: Distribution, age, sediment magnetism, and geochemistry of the Saksunarvatn (10.18 ± cal ka B.P.) ash in marine, lake, and terrestrial sediments, NW Iceland. *Journal of Quaternary Science*.
 Ashwell, I. Y., 1996: The geomorphology of Fnjoskadalur, N. Iceland: reinterpretation in terms of sub-glacial hydrologic processes, with the introduction “The Deglaciation of Iceland”. Unpublished manuscript.
 Bard, E., Arnold, M., Mangerud, J., Paterne, M., Labeyrie, L., Duprat, J., Melieres, M.-A., Sonstegaard, E., and Duplessy, J.-C., 1994: The North Atlantic atmosphere–sea surface ¹⁴C gradient during the Younger Dryas climatic event. *Earth and Planetary Science Letters*, 126: 275–287.
 Belkin, I. M., Levitus, S., Antonov, J., and Malmberg, S.-A., 1998: “Great Salinity Anomalies” in the North Atlantic. *Progress in Oceanography*, 41: 1–68.
 Birks, H. H., Gulliksen, S., Hafidason, H., Mangerud, J., and Possnert, G., 1996: New radiocarbon dates for the Vedde Ash and the

- Saksunarvatn ash from western Norway. *Quaternary Research*, 45: 119–127.
- Björck, S., Ingólfsson, O., Hafliðason, H., Hallsdóttir, M., and Anderson, N. J., 1992: Lake Torfadalsvatn: a high resolution record of the North Atlantic ash zone I and the last glacial-interglacial environmental changes in Iceland. *Boreas*, 21: 15–22.
- Bond, G. C., and Lotti, R., 1995: Iceberg discharges into the North Atlantic on millennial time scales during the last glaciation. *Science*, 267: 1005–1009.
- Bond, G., Mandeville, C., and Hoffman, S., 2001: Were rhyolitic glasses in the Vedde ash and in the North Atlantic Ash Zone 1 produced by the same volcanic eruption? *Quaternary Science Reviews*, 20: 1189–1199.
- Bourgeois, O., Dauteil, O., and Van Viet-Lanoe, B., 2000: Geothermal control on ice stream formation: flow patterns of the Icelandic Ice Sheet at the Last Glacial Maximum. *Earth Surface Processes and Landforms*, 25: 59–76.
- Cartee Schoolfield, S., 2000: Late Pleistocene sedimentation in the Denmark Strait region. Unpublished MSc thesis, University of Colorado, Boulder. 181 pp.
- Castaneda, I. S., 2001: Holocene paleoceanographic and climatic variations of the inner North Iceland continental shelf, Reykjarfjordur area. MSc, University of Colorado, Boulder, 154 pp.
- Cofaigh, C. O., and Evans, D. A., 2001: Deforming bed conditions associated with a major ice stream of the last British ice sheet. *Geology*, 29: 795–798.
- Dickson, R. R., Meincke, J., Malmberg, S., and Lee, A., 1988: The “Great Salinity Anomaly” in the northern North Atlantic 1968–1982. *Progress in Oceanography*, 20: 103–151.
- Dowdeswell, J. A., Uenzelmann-Neben, G., Whittington, R. J., and Marienfeld, P., 1994: The Late Quaternary sedimentary record in Scoresby Sund, East Greenland. *Boreas*, 23: 294–310.
- Dreimanis, A., 1979: The problems of waterlain tills. In *Moraines and Varves*, Schlüchter, C. (Ed). Zurich, A.A. Balkema, 167–177.
- Easterbrook, D. J., 1964: Void ratios bulk and densities as means of identifying Pleistocene tills. *Geological Society of America Bulletin*, 75: 745–750.
- Eiríksson, J., Simonarson, L.A., Knudsen, K.-L., and Kristensen, P., 1997: Fluctuations of the Weichselian Ice Sheet in SW Iceland: a glaciomarine sequence from Sudurnes, Seltjarnarnes, *Quaternary Science Reviews* 16: 221–240.
- Eiríksson, J., Knudsen, K.-L., Hafliðason, H., and Henriksen, P., 2000a: Late-glacial and Holocene paleoceanography of the North Iceland shelf. *Journal of Quaternary Science*, 15: 23–42.
- Eiríksson, J., Knudsen, K. L., Hafliðason, H., and Heinemeier, H., 2000b: Chronology of the late Holocene climatic events in the northern North Atlantic based on AMS ¹⁴C dates and tephra markers from the volcano, Hekla, Iceland. *Journal of Quaternary Science* 15: 573–580.
- Elliott, M., Labeyrie, L., Bond, G., Cortijo, E., Turon, J.-L., Tiseray, N., and Duplessy, J.-C., 1998: Millennial-scale iceberg discharges in the Irminger Basin during the last glacial period: relationship with the Heinrich events and environmental settings. *Paleoceanography*, 13: 433–446.
- Eyles, C. H., Eyles, N., and Miall, A. D., 1983: Lithofacies types and vertical profile models: an alternative approach to the description and environmental interpretation of glacial diamict and diamictite sequences. *Sedimentology*, 30: 393–410.
- Faugeres, J.-C., Stow, D. A. V., Imbert, P., and Viana, A., 1999: Seismic features diagnostic of contourite drifts. *Marine Geology*, 162: 1–38.
- Geirsdóttir, A., Hardardóttir, J., and Sveinbjörnsdóttir, A., 2000: Glacial extent and catastrophic meltwater events during the deglaciation of Southern Iceland. *Quaternary Science Reviews*, 19: 1749–1761.
- Geirsdóttir, A., Andrews, J. T., Olafsdóttir, S., Helgadóttir, G., and Hardardóttir, J., 2002: A 35ka B.P. record of iceberg rafting from NW Iceland: following the ice retreat from shelf to land. *Polar Research*.
- Grobe, H., 1987: A simple method for the determination of ice-rafted debris in sediment cores. *Polarforschung*, 57(3): 123–126.
- Grönvold, K., Oskarsson, N., Johnsen, S. J., Clausen, H. B., Hammer, C. U., Bond, G., and Bard, E., 1995: Ash layers from Iceland in the Greenland GRIP ice core correlated with oceanic and land sediments. *Earth and Planetary Science Letters*, 135: 149–155.
- Hafliðason, H., King, E. L., and Sejrup, H. P., 1998: Late Weichselian and Holocene sediment fluxes of the northern North Sea margin. *Marine Geology*, 152: 189–215.
- Hafliðason, H., Eiríksson, J., and Van Kreveld, S., 2000: The tephrochronology of Iceland and the North Atlantic region during the Middle and Late Quaternary: a review. *Journal of Quaternary Science*, 15: 3–22.
- Hagen, S., 1999: North Atlantic paleoceanography and climate history during the last ~70 cal. ka B.P. years. PhD dissertation, University of Tromsø, Tromsø. 110 pp.
- Håkansson, S. (1983) A reservoir age for the coastal waters of Iceland. *Geologiska Föreningens i Stockholm Förhandlingar* 105, 65–68.
- Hamilton, L. C., 1990: *Modern Data Analysis*. Pacific Grove, California, Brooks/Cole Publishing Co., 684 pp.
- Hardardóttir, J., 1999: Late Weichselian and Holocene environmental history of south and west Iceland as interpreted from studies of lake and terrestrial sediments. PhD dissertation, University of Colorado, Boulder, 332 pp.
- Hardardóttir, J., Georsdóttir, A., and Thordarson, Th., 2001: Tephra layers in a sediment core from Lake Hestvatn, southern Iceland: implications for evaluating sedimentation processes and environmental impacts on a lacustrine system caused by tephra fall deposits in the surrounding watershed. *Special Publication International Association of Sedimentology*, 30: 225–246.
- Harris, P. T., Brancolini, G., Armand, L., Busetti, M., Beaman, R. J., Giorgetti, G., Presti, M., and Trincardi, F., 2001: Continental shelf drift deposit indicates non-steady state Antarctic bottom water production in the Holocene. *Marine Geology*, 179: 1–8.
- Helgadóttir, G., 1984: Senkvartaere foraminifer og sedimenter i Faxaflói-Jokuldjupomradet Vest for Island. Unpublished thesis, University of Oslo, 116 pp. (plus appendixes).
- Helgadóttir, G., 1997: *Paleoclimate (0 to >14 ka B.P.) of W. and NW Iceland: An Iceland/USA Contribution to P.A.L.E., Cruise Report B9-97*. Reykjavik, Marine Research Institute of Iceland (not paginated).
- Hjort, C., Norddahl, H., and Ingólfsson, O., 1985: Late Quaternary geology and glacial history of Hornstrandir, Northwest Iceland: a reconnaissance study. *Jokull*, 35: 9–29.
- Hopkins, T. S., 1991: The GIN Sea. A synthesis of its physical oceanography and literature review 1972–1985. *Earth Science Review*, 30: 175–318.
- Ingólfsson, O., 1991: A review of the Late Weichselian and early Holocene glacial and environmental history of Iceland. In Caseldine, C., and Maizels, J. K. (eds.), *Environmental change in Iceland: Past and Present*. Amsterdam, Netherlands: Kluwer Academic Publishers, 13–29.
- James, E. B., 1999: Sediment analysis in Reykjafjardarall Trough, Northern Iceland. BA honors thesis, University of Colorado, Boulder. 33 pp (plus appendixes).
- Jennings, A. E., 1993: The Quaternary History of Cumberland Sound, southeastern Baffin Island: the marine evidence. *Géographie physique et Quaternaire*, 47: 21–42.
- Jennings, A. E., and Helgadóttir, 1994: Foraminiferal assemblages from the fjords and shelf of eastern Greenland. *Journal of Foraminiferal Research*, 24: 123–144.
- Jennings, A. E., and Weiner, N. J., 1996: Environmental change on eastern Greenland during the last 1300 years: evidence from foraminifera and lithofacies in Nansen Fjord, 68°N. *The Holocene*, 6: 179–191.
- Jennings, A. E., Manley, W. F., MacLean, B., and Andrews, J. T., 1998: Marine evidence for the last glacial advance across eastern Hudson Strait, eastern Canadian Arctic. *Journal of Quaternary Science*, 13: 501–514.

- Jennings, A. E., Syvitski, J. P. M., Gerson, L., Gronvald, K., Geirsdóttir, A., Hardardóttir, J., Andrews, J. T., and Hagen, S., 2000: Chronology and paleoenvironments during the late Weichselian deglaciation of the SW Iceland Shelf. *Boreas*, 29: 167–183.
- Jennings, A. E., Grönvold, K., Hilberman, R., Smith, M., and Hald, M., 2002: High resolution study of Icelandic tephra in the Kangerlussuaq Trough, SE Greenland, during the last deglaciation. *Journal of Quaternary Science*, 17: 747–757.
- Jennings, A. E., Weiner, N. J., Helgadóttir, G. and Andrews, J. T., in press: Modern foraminiferal faunas of the SW to N Iceland shelf: Oceanographic and environmental controls. *Journal of Foraminiferal Research*.
- Knudsen, K. L., and Austen, W. E. N., 1996: Late glacial foraminifera. In: Andrews, J. T., Austin, W. E. N., Bergsten, H., and Jennings, A. E. (eds.), *Late Quaternary Palaeoceanography of the North Atlantic Margins*. London: Geological Society, 7–10.
- Kovach, 1998: *Multi-Variate Statistical Package*. Pentraeth, Wales: Kovach Computing Services. 127 pp.
- Kristjansdóttir, G. B., 1999: Late Quaternary climatic and environmental changes on the North Iceland shelf. MSc thesis, University of Iceland, Reykjavik. 175 pp.
- Lamb, H. H., 1979: Climatic variations and changes in the wind and ocean circulation: the Little Ice Age in the Northeast Atlantic. *Quaternary Research*, 11: 1–20.
- Larsen, G. 2000: Holocene volcanism in Iceland and tephrochronology as a tool in volcanology. Keele University, U.K., Iceland 2000, Abstract vol., 65–67.
- Larusson, L., 1983: Aspects of the Glacial Geomorphology of the Vestfirðir Peninsula of Northwest Iceland with particular reference to the Vestur-Isafjardarsýsla area. PhD dissertation, Durham, U.K. University of Durham, 322 pp.
- Licht, K. J., Dunbar, N. W., Andrews, J. T., and Jennings, A. E., 1999: Distinguishing subglacial till and glacial marine diamictions in the western Ross Sea, Antarctica: implications for a Last Glacial Maximum grounding line. *Geological Society of America Bulletin*, 111: 91–103.
- Malmberg, S.-A., 1969: Hydrographic changes in the waters between Iceland and Jan Mayen in the last decade. *Jökull*, 19 (Symposium on Drift Ice and Climate): 30–43.
- Malmberg, S.-A., 1985: The water masses between Iceland and Greenland. *Journal of the Marine Research Institute*, 9: 127–140.
- McCave, I. N., and Tucholke, B. E., 1986: Deep current-controlled sedimentation in the western North Atlantic. In Vogt, P. R., and Tucholke, B. E. (eds.), *The Geology of North America: The Western North Atlantic Region*. Boulder, Colorado: Geological Society of America, 451–468.
- Norrdahl, H., 1991: Late Weichselian and early Holocene deglaciation history of Iceland. *Jökull*, 40: 27–50.
- Norrdahl, H., and Hafliðason, H., 1992: The Skogar Tephra, a Younger Dryas marker in North Iceland. *Boreas*, 21: 23–41.
- Olafsdóttir, T., 1975: A moraine ridge on the Iceland shelf, west of Breidafjörður. *Naturufræðingurinn*, 45: 31–37.
- Olafsson, J., 1999: Connections between oceanic conditions off N Iceland, Lake Myvatn temperature, regional wind direction variability and the North Atlantic Oscillation. *Rit Fiskideildar*, 16: 41–57.
- Piper, D. J. W., Mudie, P. J., Fader, G. B., Josenhans, H. W., MacLean, B., and Vilks, G., 1991: Quaternary Geology. In Keen, M. J., and Williams, G. L. (eds.), *Geology of the Continental Margin of Eastern Canada*. Boulder, Colorado: Geological Society of America, 475–607.
- Principato, S. M., 2000: Glacial geology of the Reykjarfjörður, NW Iceland. *Geological Society of America Abstract Volume*, 32 (7): A18–A19.
- Principato, S. M., 2003: *Late Quaternary history of eastern Vestfirðir, NW Iceland*. Ph.D. dissertation, University of Colorado, Boulder.
- Reyment, R. A., and Savazzi, E., 1999: *Aspects of Multivariate Statistical Analysis in Geology*. New York: Elsevier. 285 pp.
- Ruddiman, W. F., and McIntyre, A., 1981: The Mode and Mechanism of the Last Deglaciation: Oceanic Evidence. *Quaternary Research*, 16: 125–134.
- Rundgren, M., and Ingólfsson, O., 1999: Plant survival in Iceland during periods of glaciation? *Journal of Biogeography*, 26: 387–396.
- Rundgren, M., Ingólfsson, O., Björck, S., Jiang, H., and Hafliðason, H., 1997: Dynamic sea-level change during the last deglaciation of northern Iceland. *Boreas*, 26: 201–215.
- Sigtryggsson, H., 1972: An outline of sea ice conditions in the vicinity of Iceland. *Jökull*, 22: 1–11.
- Sjöholm, J., Serjup, H. P., and Furnes, H., 1991: Quaternary volcanic ash zones on the Iceland Plateau, southern Norwegian Sea. *Journal of Quaternary Science*, 6: 159–173.
- Smith, L. M., 2001: Holocene paleoenvironmental reconstruction of the continental shelves adjacent to the Denmark Strait. PhD dissertation, University of Colorado, Boulder. 219 pp.
- Smith, L. M., and Licht, K. J., 2000, Radiocarbon Date List IX: Antarctica, Arctic Ocean, and the northern North Atlantic. University of Colorado, Institute of Arctic and Alpine Research, Occasional Paper 54. 138 pp.
- Stefansson, U., 1969a: Near surface temperature in the Icelandic Coastal Waters. *Jökull*: 19: 29.
- Stefansson, U., 1969b: Temperature variations in the North Icelandic coastal area during recent decades. *Jökull* 19: 18–28.
- Stokes, C. R., and Clark, C. D., 2001: Palaeo-ice streams. *Quaternary Science Reviews*, 20: 1437–1457.
- Syvitski, J. P., Jennings, A. E., and Andrews, J. T., 1999: High-Resolution seismic evidence for multiple glaciation across the southwest Iceland Shelf. *Arctic and Alpine Research*, 31: 50–57.
- Syvitski, J. P. M. (ed.), 1991: *Principles, Methods, and Application of Particle Size Analysis*. Cambridge: Cambridge University Press. 368 pp.
- Turney, C. S. M., Harkness, D. D., and Lowe, J. J., 1997: The use of microtephra horizons to correlate late-glacial lake sediment successions in Scotland. *Journal of Quaternary Science*, 12: 525–531.
- Voelker, A. H. L., 1999: *Zur Deutung der Dansgaard-Oeschger Ereignisse in ultra- hochauflosenden Sedimentprofilen aus dem Europäischen Nordmeer*. Universität Kiel Report Nr. 9, Institut für Geowissenschaften. 271 pp.
- Voelker, A. H. L., Sarthein, M., Grootes, P. M., Erlenkeuser, H., Laj, C., Mazaud, A., Nadeau, M.-J., and Schleicher, M., 1998: Correlation of marine ¹⁴C ages from the Nordic Seas with the GISP2 isotope record: implications for ¹⁴C calibration beyond 25 ka BP. *Radiocarbon*, 40: 517–534.
- Vorren, T. O., Hald, M., Edvardsen, M., and Lind-Hansen, O.-W., 1983: Glacigenic sediments and sedimentary environments on continental shelves: general principles with a case study from the Norwegian shelf. In Ehlers, J. (ed.), *Glacial Deposits in North-West Europe*. Rotterdam: A. A. Balkema, 61–73.
- Wastegard, S., Björck, S., Possnert, G., and Wohlfarth, B., 1998: Evidence for the occurrence of Vedde ash in Sweden: radiocarbon and calendar age estimates. *Journal of Quaternary Science*, 13: 271–274.
- Wastl, M., Stotter, J., and Caseldine, C., 1999: Tephrochronology—a tool for correlating records of Holocene environmental and climatic change in the North Atlantic region. *Geological Society of America Abstract volume* 31: A315.
- Webb, F. M., Marshall, S. J., Björnsson, H., and Clarke, G. K. C., 1999: Modelling the variations in glacial coverage of Iceland from 120,000 BP to Present. *EOS*, abstract volume 80(40): F332.
- Weiner, N., Helgadóttir, G., and Jennings, A. E., 1999: Modern foraminiferal faunas of the western and northern Iceland Shelf. *Geological Society of America. Abstract volume*, 31(7): A315.

Ms submitted February 2002

Revised ms submitted August 2002